Int. J. Advance Soft Compu. Appl, Vol. 11, No. 2, July 2019
ISSN 2074-8523

Road Surface Types Classification Using Combination of K-Nearest Neighbor and Naïve Bayes Based on GLCM

Susi Marianingsih[1], Fitri Utaminingrum[1], and Fitra Abdurrachman Bachtiar[1]

[1] Faculty of Computer Science, Brawijaya University, Malang, Indonesia
e-mail: ssmarianingsih@student.ub.ac.id, f3_ningrum@ub.ac.id, fitra.bachtiar@ub.ac.id

Abstract

The automatic capability of determining the road surface type is essential information for autonomous vehicle navigation such as wheelchair and smart car. This factor is crucial because determining the type of road surface can increase security for auto vehicle users. This study used texture information to extract features from pictures using Gray Level Co-occurrence Matrix (GLCM), and combine K-Nearest Neighbor classifier (KNN) and Naïve Bayes classifier (NB) to characterize surface objects into three road classes, i.e., asphalt, gravel, and pavement. The combination of 2 classification methods is then written as KNB. The classification performance of KNB will compare with another classifier. In this study, there were 750 images of original roads (asphalt, gravel, and Pavement) that were arranged into a dataset. The results show that the classification accuracy using KNB is higher than the comparison classification methods.

Keywords: *classification, road surface texture, GLCM, KNN, Naïve Bayes.*

1 Introduction

At present, vehicle comfort and safety are very important factors for automotive manufacturers and the government when they want to recognize road conditions [1][2]. This factor is very important because it can help drivers and smart vehicle control systems, and it can also be indicators and alarms for repair processes and road maintenance schedules [2] - [5]. On the other hand, the type of road surface is the first critical information for users of automatic vehicles such as smart wheelchairs [6] or smart cars because it can improve the safety of automatic vehicle

users. A crucial factor that can be used by users to find out the type of road surface is information about road texture.

Haralick features are commonly used by researchers for feature extraction, and to catch on texture information in images, researchers often use the pixel intensity of local spatial variations. Furthermore, Haralick et al. [7] proposed to use the GLCM method to describe texture features in the spatial domain. GLCM Matrix examines texture by considering the spatial relationship of pixels. GLCM functions characterized image textures by calculating the appearance of a pixel pair with a specific value and in a particular spatial relationship. Thus, the GLCM matrix is made to extract the statistical measurements of an image. Zhang et al.[8], using GLCM for edge images and Prewitt edge detectors applied there in four directions. Palm [9] uses GLCM on color channel information LUV and RGB to extract features from images, and Partio et al. [10] using GLCM to determine the texture features of rock images. Besides [11], [12] also uses the GLCM application. Moreover, to represent the color and intensity of the pixel environment in the picture, the GLCM method has also been used by Vadivel et al.[13]. Color spatial co-relation is used in color correlogram [14], then [15] has combined color correlation and supervised learning methods to extract features from the image. Pass et al. [16] comparing color coherence and color histogram for image selection. In addition, by combining HSV histograms and entropy values from the GLCM matrix, it produces a feature vector for image grouping using Artificial Neural Networks introduced by Park et al. [17]Gaussian Mixture Vector Quantization uses an image feature of color histogram quantization for the retrieval image process [18]. Jhanwar et al. [19] introduce a Co-occurrence Matrix Motif to image selection. Changing the Color of the Co-occurrence Motive Matrix [20] is the development of a Co-occurring Motif Matrix that uses color channel relationships.

On the other hand, Popescu et al. [21] state that through the road types obtained from visual data the road surface can be classified based on the texture features obtained from the GLCM road image. Furthermore, Tang et al. [22] also classify using colors, textures, and edge features of the limited sub-region of the driving perspective to training road-type neural networks, and Slavkovikj et al. [23] proposed a content-based method for classifying road types with unattended image learning.

Furthermore, to improve accuracy, some researchers combine KNN and NB. Dynamic K-Nearest-Neighbors Naive Bayes with importance properties proposed by Jiang et al. [23]. Hsiao et al. [24] using hybrid KNN and NB for predicting subcellular locations of eukaryotic proteins. McCann and Lowe [25] propose Local Naive Bayes Nearest Neighbors to classify pictures. Ferdousy et al. [26] combine the distance-based algorithm K-Nearest Neighbours and statistically based NB Classifier. They use K-Nearest Neighbours to classify numerical attribute and Naïve Bayes to classify categorical attribute. From these studies, it shows that the combined KNN and NB are accurate in solving classification problems. Unfortunately, they haven't revealed the determination of road surface type.

Besides, determination of road surface type is critical, so that still require intensive investigation, especially to improve security for auto vehicle users. Therefore, in this study, we focused on the combination of KNN and NB to classify road surface types. The type of road surface is classified as asphalt, gravel, and pavement.

The composition of the script consists of several sections. In section 2 is about the road surface dataset. Section 3 contains details of feature texture extraction, KNN, and NB, including the proposed method, and on section 4 contains the results and discussion. The last one is section 5 containing the conclusions of this study.

2 Road Surface Dataset

We build a dataset from surface images of the small road (see Figure 1a, 1b, and 1c). The dataset is arranged from 210 road images with proper illumination from Instant Google Street View [27], and form Figure 1, we can see that the road is divided into three categories: asphalt road (70 images), gravel road (70 images), and pavement road (70 images).

(a) (b) (c)

Fig. 1. The types of road objects
(a) asphalt, (b) gravel, and (c) pavement.

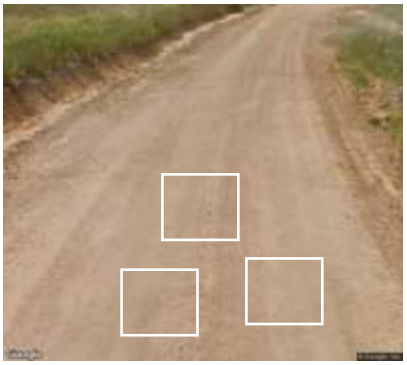

Fig. 2. Sub-pictures caught from the object.

From figure 2 we can see that we captured 100 x 100 sub-pictures from the object surfaces to make the dataset. Overall, from figure 3, it can be seen that in the dataset there are 750 pictures of the road surface, 600 pictures data training, and 150 pictures data test.

(a) (b) (c)

Fig. 3. The type of surface object pictures was taken from (a) asphalt, (b) gravel, and (c) pavement road.

3 Methodology

3.1 Gray level co-occurrence matrix texture features

The gray level co-occurrence matrix is one of the popular texture feature extraction methods proposed by Haralick et al. [28]. This method calculates the possibility of a close relationship between two pixels at a certain angular distance and orientation, then forms a co-occurrence matrix of image data, and continues to define features as a function of the intermediate matrix.

The formation of the co-occurrence matrix is described in Figure 4. A sample matrix of image pixels (Figure 4(a)), GLCM is counted for the matrix (a), and in the GLCM matrix (Figure 4(b)) the top row and leftmost column are the pixel values in the matrix (a). For each pair ((0,0),(0,1),(0,2),…), co-occurrence has been calculated. For example, pixels pair (0,0) with the direction of 0^o (horizontal pixel pair) and one range (adjacent pair), just two times as displayed with a blue circle around it in the image. Hence, at point (0,0) number '2' occurred in GLCM. In like manner, different elements of GLCM are calculated. This research use 0^o, 45^o, 90^o, and 135^o in the direction of the pixel pair (see Figure 4(c)).

After obtaining the co-occurrence matrix, the process continued to compute a second-order statistical feature that represents the observed image. Furthermore, to extract various types of texture characteristics it can be obtained from the co-occurrence matrix [28], and for reducing the computing time, this study only uses some features i.e., Angular Second-Moment (ASM), entropy, contrast, and correlation.

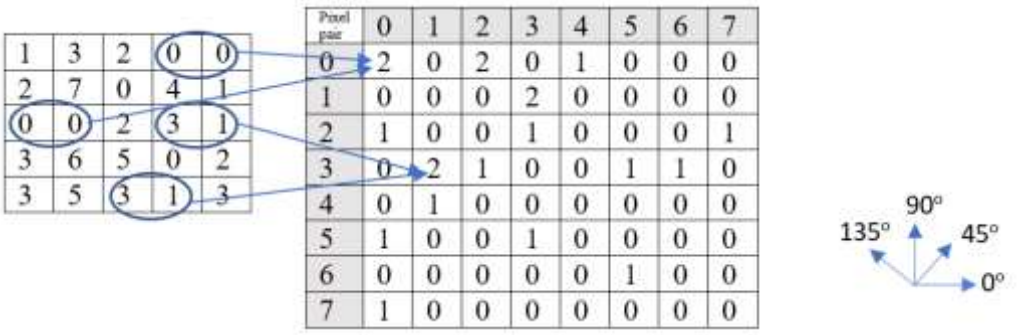

(a) (b) (c)

Sample of image pixels Co-occurrence matrix Direction of pixel pair

Fig. 4. The calculation example of the Gray level co-occurrence matrix.

To find out the dimensions of a homogeneity image by using the Angular Second-Moment Feature (ASM) parameter, whereas to find out the gray level irregularities in the image using the entropy feature parameter. In addition, the parameters used to find out the different moments of the GLCM matrix and the contrast size or the amount in the image are contrast features. Whereas, for linear-gray-dependency in images can be measured using the correlation feature. Therefore, the equation features considered are:

$$ASM = \sum_{i=1}^{n} \sum_{j=1}^{n} \{P(i,j)\}^2 \tag{1}$$

$$Entropy = -\sum_{i=1}^{n} \sum_{j=1}^{n} P(i,j) \log\{P(i,j)\} \tag{2}$$

$$Contrast = \sum_{i=1}^{n} \sum_{j=1}^{n} (i-j)^2 P(i,j) \tag{3}$$

$$Correlation = \frac{\sum_{i=1}^{N} \sum_{j=1}^{N} (ijP(i,j)) - \mu_x \mu_y}{\sigma_x \sigma_y} \tag{4}$$

Where *P(i,j)* is an element of the co-occurrence matrix on the *i*-row and the *j*-column. The means (μ_x, μ_y) and variances (σ_x, σ_y) are given by:

$$\mu_x = \sum_{i=1}^{n} i \sum_{j=1}^{n} P(i,j) \tag{5}$$

$$\mu_y = \sum_{j=1}^{n} j \sum_{i=1}^{n} P(i,j) \tag{6}$$

$$\sigma_x = \sum_{i=1}^{n} (j-\mu_x)^2 \sum_{j=1}^{n} P(i,j) \tag{7}$$

$$\sigma_y = \sum_{j=1}^{n} (j-\mu_y)^2 \sum_{i=1}^{n} P(i,j) \tag{8}$$

3.2 K-Nearest Neighbor Classifier (KNN)

K-NN classifier is a simple algorithm and type of instance-based learning was based on the size of the similarity (e.g., the function of distance) then all cases are stored and classified as a new case.
On the other hand, based on the most votes from neighbors, a case can be classified, with cases assigned to the class most common among their closest neighbors. If k=1, then a simple case is assigned to the nearest neighbor class. We use Euclidean distance functions, and the equation is:

$$d = \sqrt{\sum_{i=1}^{k}(x_i - y_i)^2} \tag{9}$$

3.3 Naïve Bayes Classifier (NB)

Naive Bayes classifier is so easy and more efficient linear classifier, in which the shape of the road surface is classified into three clusters *(Ci)*, namely: asphalt *(C1)*, gravel *(C2)* and pavement surface *(C3)*.

In this section, we pattern a Naïve Bayes classifier. Each selected image is represented as an n-metrical vector $F = \{f1, f2, \ldots, fn\}$. Furthermore, with The Bayesian classifier will classify a test sample *F* classified into cluster *Ci* if and only if.

$$P(C_i \mid F) > P(C_j \mid F), \quad 1 \leq j \leq m, j \neq i \tag{10}$$

From the Bayesian theory,

$$P(C_i \mid F) = P(C_i \mid F_1, F_2, \ldots, F_n) = \frac{P(F \mid C_i)P(C_i)}{P(F)} \tag{11}$$

$P(C_i \mid F)$ is the posterior probability of cluster C_i gave feature $(f_1, f_2, \ldots, f_n)$. $P(C_i)$ is the prior probability of cluster C_i and $P(F)$ is the prior probability of properties $(f_1, f_2, \ldots, f_n)$. This is adequate to select the category for maximizes the equation:

$$P(X \mid C_i) = \prod_{k=1}^{n} P(x_k \mid C_i) \tag{12}$$

To represent conditional-class probabilities, we use a Gaussian distribution. For the continued variable, we consider a pattern of possibility for continued features. The allocation is described by variables mean (μ) with variation (σ). For every cluster *Cj*, the cluster-conditional possibility for symbol *fi* is:

$$P(F = f_i \mid C = c_j) = \frac{e^{-\frac{(x_i - \mu_{ij})^2}{2\sigma_{ij}^2}}}{\sqrt{2\pi\sigma_{ij}}} \tag{13}$$

The parameter mean (μ_{ij}) can be calculated based on the sample mean of $F(f_i)$ for all training records that belong to the cluster y_j, and the standard deviation (σ_{ij}^2) can be calculated from the sample variance of such training records.

$$\mu_{ij} = \frac{1}{n}\sum_{k=1}^{n} f_k \tag{14}$$

$$\sigma_{ij} = \sqrt{\frac{1}{(n-1)}\sum_{k=1}^{n}(f_k - \mu_{ij})^2} \tag{15}$$

Finally, the posterior possibilities are calculated for every cluster, and predictions are made on clusters that have maximum posterior possibilities. The estimated class ($\hat{C}_i$) correlated with F is:

$$\hat{C}_i = max\, P(C_i|F(f_1, f_2, \dots, f_n) \tag{16}$$

3.4 Proposed Method

In this study, we combined the KNN and NB methods (in short, we write as KNB). The KNB classifier describes as follow:
Step 1: using KNN classifier to get K-Nearest Neighbor from training data.
Step 2: Next, using K-Nearest data as training data for the NB classifier, and in figure 5 we display a system block diagram.

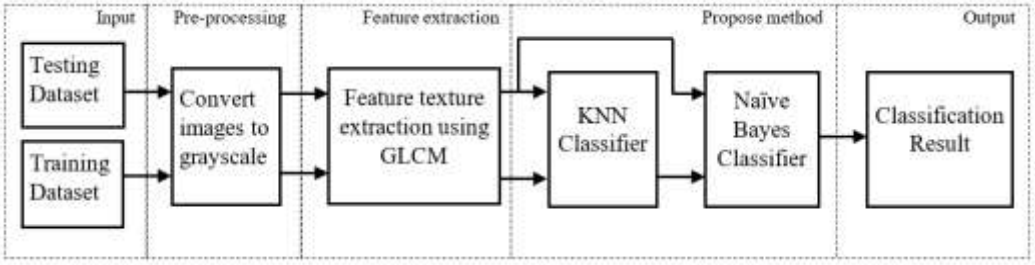

Fig. 5. System block diagram

4 Results

4.1 Performance Measurements

The performance measurements used for this research were a recall, precision, classifier F1 ranking and precision [29],[30]. In Table 1, we calculate using the Confusion Matrix as a predictive classification table.

Table 1. Confusion Matrix

		Predictive	
		Irrelevant	Relevant
Actual	Irrelevant	*TN*	*FP*
	Relevant	*FN*	*TP*

The amount of right predictions of an irrelevant object is called True Negative (TN), the sum of right predictions of relevant object is False Positive (FP), and the sum of prediction errors found on an irrelevant object is called False Negative (FN), and the sum of valid predictions where an interconnected object is called True Positive (TP). The measurements formulation we use are:

$$Recall = \frac{TP}{FN+TP} \tag{17}$$

$$Precision = \frac{TP}{FP+TP} \tag{18}$$

$$F - Measure = \frac{2\ x\ Recall\ x\ Precision}{Recall+Precision} \tag{19}$$

$$Accuracy = \frac{TN+TP}{TN+FN+TP+FP} \tag{20}$$

4.2 Result and discussion

In Figure 3, we use the road pictures dataset provide of 750 pictures divided to a set training of 600 pictures (200 pictures per category) and a testing set of 150 pictures (50 pictures per category). Measuring Co-occurrence matrices for all pictures of the dataset. Features ASM, entropy, contrast and correlations are measured of every co-occurrence matrix. Features value are saving in the property vector from the appropriate picture. These features are input for classification methods. The performance measurements used for this research were recall, precision, f-measure, and accuracy.

The first experiment to determine the value of k with the highest classification accuracy. The experiment results in k value are shown in Figure 6. The experiment shows that value of k = 200 and k = 300 provide the best performance with accuracy 0.89.

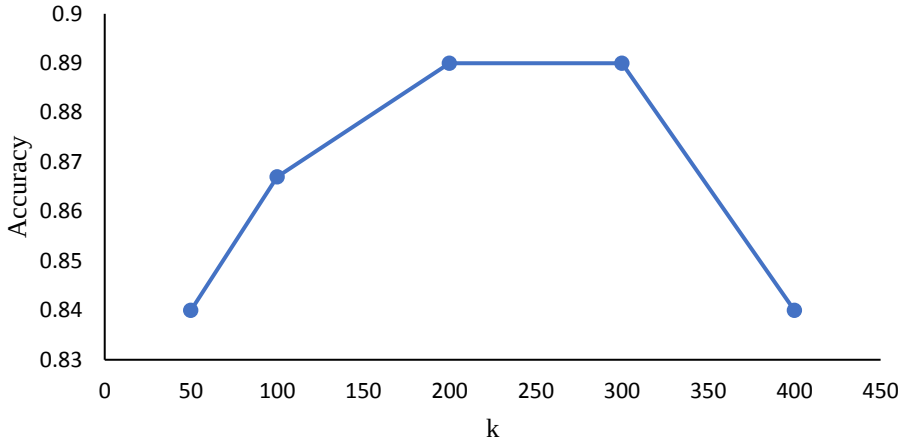

Fig. 6. Accuracy of KNB based on k value

The KNB classifier compared with KNN and NB. The confusion matrix in Table 1 displays the classification output of 3 methods. The bold value in Table 2 shows the amount of data that is classified correctly. For each class, recall, precision, f-measure, and accuracy on KNB tend to be greater than KNN and NB. This shows that KNB is higher than KNN and NB, Table 3 and Table 4.

We also compare KNB with other classification methods (see Table 5), Ferdousy et al. [27], Lee [31], McCann and Lowe [26], and Timofte et al. [32]. The results of the comparison show that each method produces different accuracy, where cNK has an accuracy of 0.859, NB-KNN 0.684, Local NBNN 0.719, NBNN5 0.743. However, our results found that with KNB the accuracy is 0.89 higher than other methods. This phenomenon indicates that KNB has the potential to be used in other datasets.

Table 2. Confusion Matrix

Classifier	Class	Data Testing	Experiment Result		
			Asphalt	Gravel	Pavement
KNB	Asphalt	50	**45**	1	4
	Gravel	50	0	**48**	2
	Pavement	50	6	4	**40**
KNN	Asphalt	50	**46**	1	3
	Gravel	50	0	**39**	11
	Pavement	50	3	8	**39**
NB	Asphalt	50	**46**	1	3
	Gravel	50	0	**24**	26
	Pavement	50	9	2	**39**

Table 3. Performance Measurements

Classifier	Class	Precision	Recall	F-measure
KNB	Asphalt	0,92	0,9	0,91
	Gravel	0,87	0,96	0,91
	Pavement	0,87	0,8	0,83
KNN	Asphalt	0,94	0,92	0,93
	Gravel	0,81	0,78	0,8
	Pavement	0,74	0,78	0,76
NB	Asphalt	0,84	0,92	0,88
	Gravel	0,89	0,48	0,62
	Pavement	0,57	0,78	0,66

Table 4. Accuracy of three methods

Classifier	Accuracy
KNN	0,81
NB	0,73
KNB	0,89

Table 5. Comparison with previous studies

Method	Dataset	Accuracy
cNK [26]	Heart disease	0,859
NB-KNN [31]	Emo-DB	0,684
Local NBNN [25]	Caltec 101	0,719
$NBNN_5$ [32]	Scene-15	0,743
KNB [Present study]	Road Surface Images	0,89

5 Conclusion

A study using the KNB method and comparing it with KKN and NB method has been done, and the KNB method has better accuracy than KNN and NB to determine the road surface type. This is because KNN can find some data that is the closest to the data test so that NB successfully increases its ability to classify road surfaces. The results show that the KNB's accuracy reaches 0.89 and has the opportunity to be increased by considering other factors. Moreover, when compared with other methods (cNK, NB-KNN, Local NBNN, $NBNN_5$) it is shown that KNB is better than other methods because it has higher accuracy. This phenomenon indicates that the KNB has the potential to calculate the accuracy of different datasets. Because KNB has positive results, it is necessary to do further research using color and texture features.

ACKNOWLEDGMENTS
This research was supported by Research Group of the Computer Vision, Engineering Department of Informatics, Faculty of Computer Science, the University of Brawijaya.

References

[1] Z.-F. Wang, M.-M. Dong, L. Gu, J.-J. Rath, Y.-C. Qin, and B. Bai, "Influence of Road Excitation and Steering Wheel Input on Vehicle System Dynamic Responses," *Applied Sciences*, vol. 7, no. 6, p. 570, Jun. 2017.

[2] Y. Qin, Z. Wang, C. Xiang, E. Hashemi, A. Khajepour, and Y. Huang, "Speed independent road classification strategy based on vehicle response: Theory and experimental validation," *Mechanical Systems and Signal Processing*, vol. 117, pp. 653–666, Feb. 2019.

[3] Z. Li, I. V. Kolmanovsky, E. M. Atkins, J. Lu, D. P. Filev, and Y. Bai, "Road Disturbance Estimation and Cloud-Aided Comfort-Based Route Planning," *IEEE Transactions on Cybernetics*, vol. 47, no. 11, pp. 3879–3891, Nov. 2017.

[4] C. Hu, R. Wang, F. Yan, Y. Huang, H. Wang, and C. Wei, "Differential Steering Based Yaw Stabilization Using ISMC for Independently Actuated Electric Vehicles," *IEEE Transactions on Intelligent Transportation Systems*, vol. 19, no. 2, pp. 627–638, Feb. 2018.

[5] C. Gorges, K. Öztürk, and R. Liebich, "Impact detection using a machine learning approach and experimental road roughness classification," *Mechanical Systems and Signal Processing*, vol. 117, pp. 738–756, Feb. 2019.

[6] F. Utaminingrum *et al.*, "A laser-vision based obstacle detection and distance estimation for smart wheelchair navigation," 2016, pp. 123–127.

[7] R. M. Haralick, K. Shanmugam, and I. Dinstein, "Textural Features for Image Classification," *IEEE Transactions on Systems, Man, and Cybernetics*, vol. SMC-3, no. 6, pp. 610–621, Nov. 1973.

[8] J. Zhang, G. Li, and S. He, "Texture-Based Image Retrieval by Edge Detection Matching GLCM," 2008, pp. 782–786.

[9] C. Palm, "Color texture classification by integrative Co-occurrence matrices," *Pattern Recognition*, vol. 37, no. 5, pp. 965–976, May 2004.

[10] M. Partio, M. Gabbouj, and A. Visa, "Rock texture retrieval using gray level co-occurrence matrix," *Proc. 5th Nord. Signal …*, 2002.

[11] A. Baraldi and F. Parmiggiani, "An investigation of the textural characteristics associated with gray level co-occurrence matrix statistical parameters," *IEEE Transactions on Geoscience and Remote Sensing*, vol. 33, no. 2, pp. 293–304, Mar. 1995.

[12] V. Kovalev and M. Petrou, "Multidimensional Co-occurrence Matrices for Object Recognition and Matching," *Graphical Models and Image Processing*, vol. 58, no. 3, pp. 187–197, May 1996.

[13] A. Vadivel, S. Sural, and A. K. Majumdar, "An Integrated Color and Intensity Co-occurrence Matrix," *Pattern Recognition Letters*, vol. 28, no. 8, pp. 974–983, Jun. 2007.
[14] Jing Huang, S. R. Kumar, M. Mitra, Wei-Jing Zhu, and R. Zabih, "Image indexing using color correlograms," 1997, pp. 762–768.
[15] J. Huang, S. R. Kumar, and M. Mitra, "Combining supervised learning with color correlograms for content-based image retrieval," 1997, pp. 325–334.
[16] G. Pass, R. Zabih, and J. Miller, "Comparing images using color coherence vectors," 1996, pp. 65–73.
[17] S. Park, K. Seo, and D. Jang, "Expert system based on artificial neural networks for content-based image retrieval," *Expert Systems with Applications*, vol. 29, no. 3, pp. 589–597, Oct. 2005.
[18] S. Jeong, C. S. Won, and R. M. Gray, "Image retrieval using color histograms generated by Gauss mixture vector quantization," *Computer Vision and Image Understanding*, vol. 94, no. 1–3, pp. 44–66, Apr. 2004.
[19] N. Jhanwar, S. Chaudhuri, G. Seetharaman, and B. Zavidovique, "Content-based image retrieval using motif co-occurrence matrix," *Image and Vision Computing*, vol. 22, no. 14, pp. 1211–1220, Dec. 2004.
[20] M. Subrahmanyam, Q. M. Jonathan Wu, R. P. Maheshwari, and R. Balasubramanian, "Modified color motif co-occurrence matrix for image indexing and retrieval," *Computers & Electrical Engineering*, vol. 39, no. 3, pp. 762–774, Apr. 2013.
[21] Dan Popescu, Radu Dobrescu, Daniel Merezeanu, "Road Analysis Based On Texture Similarity Evaluation," *Proceedings of the 7th WSEAS International Conference on SIGNAL PROCESSING (SIP'08)*, May 2008.
[22] Isabelle Tang and Toby P. Breckon, "Automatic Road Environment Classification," *IEEE TRANSACTIONS ON INTELLIGENT TRANSPORTATION SYSTEMS*, vol. VOL. 12, Jun. 2011.
[23] L. Jiang, H. Zhang, and Z. Cai, "Dynamic K-Nearest-Neighbor Naive Bayes with Attribute Weighted," in *Fuzzy Systems and Knowledge Discovery*, vol. 4223, L. Wang, L. Jiao, G. Shi, X. Li, and J. Liu, Eds. Berlin, Heidelberg: Springer Berlin Heidelberg, 2006, pp. 365–368.
[24] Hsiao, H. C. W., Chen, S., Chang, J. P., & Tsai, J. J. P., "Subcellular Locations of Eukaryotic Proteins Using Bayesian and K-Nearest Neighbor Classifiers," *Journal of Information Science and Engineering*, vol. 24, no. 5, pp. 1361–1375, 2008.
[25] Sancho McCann, David G. Lowe, "Local Naive Bayes Nearest Neighbor for Image Classification," *CVPR*, 2012.
[26] E. Z. Ferdousy, M. M. Islam, and M. A. Matin, "Combination of Naïve Bayes Classifier and K-Nearest Neighbor (cNK) in the Classification Based Predictive Models," *Computer and Information Science*, vol. 6, no. 3, May 2013.
[27] "https://www.instantstreetview.com/," 2018.

[28] R. M. Haralick, K. Shanmugam, and I. Dinstein, “Textural Features for Image Classification,” *IEEE Transactions on Systems, Man, and Cybernetics*, vol. SMC-3, no. 6, pp. 610–621, Nov. 1973.
[29] Powers, D.M.W., “Evaluation: From Precision, Recall And F-Measure To Roc, Informedness, Markedness & Correlation,” *Journal of Machine Learning Technologies*, 2011.
[30] I. K. Somawirata and F. Utaminingrum, “Road detection based on the color space and cluster connecting,” 2016, pp. 118–122.
[31] S. Lee, “Hybrid Naïve Bayes K-nearest neighbor method implementation on speech emotion recognition,” in *2015 IEEE Advanced Information Technology, Electronic and Automation Control Conference (IAEAC)*, Chongqing, China, 2015, pp. 349–353.
[32] Radu Timofte1, Tinne Tuytelaars1, and Luc Van Gool1, “Naive Bayes Image Classification: beyond Nearest Neighbors,” *Proceedings of 11th Asian conference on computer vision*, Nov. 2012.